ISSN: 1410-8917
Jurnal Kimia Sains & Aplikasi
e-ISSN: 2597-9914

Jurnal Kimia Sains dan Aplikasi 28 (3) (2025): 155-167

Jurnal Kimia Sains dan Aplikasi
Journal of Scientific and Applied Chemistry

Journal homepage: http://ejournal.undip.ac.id/index.php/ksa

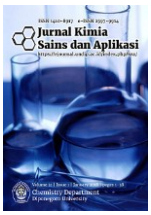

In Silico Study of Corn Silk Luteolin (*Zea mays* L.) Derivatives as Potential Antihypertensive Agents

Richa Mardianingrum [1,*], Yuli Fitriani [1], Srie Rezeki Nur Endah [1], Ruswanto Ruswanto [2]

[1] Department of Pharmacy, Faculty of Health Sciences, Perjuangan University, Tasikmalaya, Indonesia
[2] Faculty of Pharmacy, Universitas Bakti Tunas Husada, Tasikmalaya, Indonesia

* Corresponding author: richamardianingrum@unper.ac.id

https://doi.org/10.14710/jksa.28.3.155-167

Article Info

Article history:

Received: 04th December 2024
Revised: 13th April 2025
Accepted: 15th April 2025
Online: 30th April 2025

Keywords:
antihypertensive; angiotensin; in silico; lisinopril; *Zea mays* L.

Abstract

Hypertension is a condition where the systolic blood pressure is > 140 mmHg and the diastolic pressure is > 90 mmHg. Hypertension is caused by the formation of angiotensin II from angiotensin I by Angiotensin Converting Enzyme (ACE). Lisinopril is one of the drugs commonly used to treat hypertension; however, long-term use may be associated with carcinogenic effects. This study aims to find candidates for new medicinal ingredients from luteolin derivative compounds contained in corn silk (*Zea mays* L.) as antihypertensives that have the activity of inhibiting ACE enzymes. Molecular docking and molecular dynamics simulations were employed in this study. The results showed that the TL59 compound exhibited lower predicted toxicity than lisinopril. Based on molecular dynamics analysis, TL59 demonstrated an RMSD value of 1 Å and a ΔG_{TOTAL} of − 44.65 kcal/mol, whereas lisinopril showed an RMSD value of 1.3 Å and a ΔG_{TOTAL} of −29.25 kcal/mol. These findings suggest TL59 has a higher binding affinity and greater stability toward the 1086 receptor than lisinopril. Therefore, TL59 is predicted to be a promising candidate for a new antihypertensive drug that inhibits the conversion of angiotensin I to angiotensin II. In conclusion, TL59 demonstrates strong binding affinity and pharmacokinetic properties, indicating its potential as a promising antihypertensive candidate. However, this study is limited to in silico analysis and requires further in vitro and in vivo validation to confirm its efficacy and safety.

1. Introduction

Hypertension is a vascular disorder characterized by an increase in blood pressure above the normal threshold, defined as a systolic pressure greater than 140 mmHg and a diastolic pressure greater than 90 mmHg, confirmed by two separate measurements at different times [1]. According to data from the World Health Organization (WHO) [2], hypertension is a critical health issue that requires immediate attention. It is estimated to affect 22% of the global population, with the highest prevalence observed in the African region (27%), followed by the Eastern Mediterranean (26%) and Southeast Asia (25%).

According to the Indonesian Ministry of Health [3], the prevalence of hypertension in Indonesia is 34.1%, with rates of 21.20% among the pre-elderly (ages 45–59 years) and 32.5% among the elderly (aged 60 years and above). West Java Province ranks fourth among regions with the highest prevalence of hypertension, at 29.4%. Within West Java, the districts and cities with the highest reported prevalence rates are Bogor City (101.9%), Cirebon City (99.7%), Sumedang Regency (98.7%), and Tasikmalaya Regency/City (13.5%) [4].

Hypertension can generally be managed through diet, exercise, and synthetic drug therapy, one of which is lisinopril, a drug known for its antihypertensive effect through inhibition of the angiotensin-converting enzyme (ACE). ACE is responsible for converting angiotensin I into angiotensin II, a potent vasoconstrictor that also stimulates aldosterone secretion [5]. However, long-term use of lisinopril has been widely reported to cause side effects such as coughing, nausea, vomiting, dizziness, headaches, and hepatotoxicity [6].

The contribution of ACE to hypertension is part of the renin-angiotensin-aldosterone system (RAAS), a critical regulatory pathway for blood pressure and fluid balance. In this system, renin secreted by the kidneys converts angiotensinogen into angiotensin I, which is then activated to angiotensin II by ACE. Angiotensin II increases vascular resistance through vasoconstriction and promotes sodium and water retention by stimulating aldosterone release, leading to elevated blood pressure.

Therefore, inhibiting ACE reduces the formation of angiotensin II, promotes vasodilation, decreases blood volume, and ultimately lowers blood pressure, making ACE a key therapeutic target in the management of hypertension. However, considering the side effects associated with current ACE inhibitors such as lisinopril, there is a need to explore alternative agents with similar inhibitory potential but improved safety profiles. Corn silk (*Zea mays* L.) is a promising natural source that contains bioactive compounds reported to exhibit ACE inhibitory activity [7]. By targeting ACE, these compounds could interfere with the RAAS, a critical regulator of blood pressure and fluid balance.

Moreover, inhibiting ACE disrupts the conversion of angiotensin I into angiotensin II, a potent vasoconstrictor, promoting aldosterone secretion, leading to sodium and water retention. As a result, ACE inhibition not only reduces vascular resistance but also decreases blood volume, thereby offering an effective strategy for lowering blood pressure. This mechanism forms the basis for the therapeutic application of ACE inhibitors in hypertension management.

Empirically, corn has been traditionally used by people in Eastern Indonesia as an antihypertensive and antidiabetic agent [8]. Corn silk contains several secondary metabolites, including alkaloids, flavonoids, and saponins, contributing to its potential as an antihypertensive agent [9]. Among these, flavonoid compounds such as luteolin, quercetin, rutin, kaempferol, rhoifolin, and apigenin have been reported to exhibit ACE inhibitory activity [10]. Previous in vivo studies have demonstrated that the infusion of a combination of corn silk and kernels (1:1) effectively reduced systolic and diastolic blood pressure in male rats [11].

Additionally, a 260 mg/kg BW dose of corn silk water extract has been shown to lower blood pressure in 20 individuals with hypertension, partly attributed to its potassium-induced diuretic action [12]. Furthermore, an ethanol extract of corn silk and kernels at a dose of 500 mg/kg BW was found to reduce systolic blood pressure by 20.04 mmHg and diastolic pressure by 13.16 mmHg in rats with MSG-induced hypertension [7]. Luteolin, in particular, has been shown to inhibit ACE activity in MSG-induced hypertensive mice [13].

Given these findings, further research is needed to identify active compounds derived from luteolin in corn silk (*Zea mays* L.) that may possess potent antihypertensive activity. One promising approach is through in silico studies, which involve computational techniques and data analysis to facilitate the exploration of drug candidates [14]. Therefore, this study aims to identify luteolin derivative compounds that meet toxicity and pharmacokinetic criteria and to investigate their interactions with the ACE receptor in silico, with the goal of discovering new candidate compounds with strong antihypertensive potential.

2. Experimental

2.1. Tools and Materials

The tools used in this study included both hardware and software. The hardware consisted of a personal computer with the following specifications: processor - AMD A6-9220 RADEON R4, 5 COMPUTE CORES (2C+3G) 2.50 GHz; installed RAM - 4.00 GB; system type - 64-bit operating system, x64-based processor; and device ID - C213A3F6-5BBD-4EEE-B5A9-B950A2F5EB9A. The software used included ChemDraw Ultra 8.0, AutoDockTools, MarvinSketch, Discovery Studio Visualizer, Molegro Molecular Viewer, PyRx, and various databases such as the Protein Data Bank (PDB), PubChem, and PDBsum. Additionally, toxicity and pharmacokinetics analysis were conducted based on Lipinski's Rule of Five.

The materials employed in this study were 100 molecules of the corn silk luteolin derivative compound as the ligand, lisinopril as the reference compound, and the ACE receptor, obtained from the PDB with the code 1O86 [15].

2.2. Ligand Preparation

Ligands downloaded from PubChem were prepared by protonation and conformational adjustment using the MarvinSketch application. The protonation step was performed by selecting Tools > Protonation > Major Microspecies > OK. The pH was then adjusted to 7.4, which is the physiological pH of the body, and the file was saved in .mrv format. Subsequently, the conformation step was executed by selecting Tools > Conformation > Conformers > Save, and the file was saved in .mol2 format.

2.3. Receptor Preparation

The ACE receptor was first downloaded from the RCSB PDB website (http://www.rcsb.org/pdb/) using receptor code 1O86. In AutodockTools, the receptor file was opened by selecting File > Read Molecule, followed by removing the water compound through Edit > Delete Water. Next, hydrogen atoms were added using Edit > Add Hydrogen > Polar Only > OK, and the file was saved in .pdb format. The receptor was then processed using Molegro Molecular Viewer by opening the file via File > Import Molecules, selecting only the protein section, and saving the receptor with Export Molecules > Export > Save .pdb [16].

2.4. Toxicity and Pharmacokinetics

Toxicity and pharmacokinetic tests for luteolin and its derivatives were conducted using the PreADMET web server. For ADME testing, the PreADMET site was accessed, the ligand was uploaded, and the submission was completed. For toxicity testing, the Toxicity section of the PreADMET site was accessed, the ligand was

uploaded, and the submission was completed [17]. The parameters analyzed in the toxicity test included the Ames Test, Carcinogenicity in Mice, and Carcinogenicity in Rats. The pharmacokinetic parameters evaluated included Caco-2 permeability, Human Intestinal Absorption (HIA), and Plasma Protein Binding (PBB).

2.5. Screening Ligand-Based Drugs Likeness (Drug Scan)

Drug scan testing was conducted on the test compound, luteolin, and its derivatives to evaluate their physicochemical properties using Lipinski's Rule of Five web server (http://www.scfbio-iitd.res.in/software/drugdesign/lipinski.jsp) by following the steps: select file → click ligand → open → submit [16]. The parameters analyzed included molecular weight, log P value, number of hydrogen bond donors, number of hydrogen bond acceptors, and molar refractivity [18].

2.6. Docking Validation

Validation was performed by first separating the receptor and then re-docking it with the natural ligand using AutoDock Tools. If the Root Mean Square Deviation (RMSD) obtained from the re-docking process was less than 2 Å, the method was considered valid [16].

2.7. Molecular Docking

Molecular docking was performed using PyRx version 0.8, which integrates AutoDock Vina for docking simulations. The 3D structures of the ligands (luteolin derivatives and lisinopril as the reference) were first prepared by optimizing their geometry, adjusting protonation states to physiological pH (7.4), and converting them into PDBQT format. The target protein, ACE (PDB ID: 1086), was retrieved from the Protein Data Bank and preprocessed by removing water molecules and co-crystallized ligands, adding polar hydrogens, and assigning Kollman charges using AutoDock Tools. A docking grid box was centered on the enzyme's active site, with dimensions set at 40 × 40 × 40 Å to fully cover the binding pocket. Docking simulations were conducted to identify the most stable ligand conformations based on binding affinity (ΔG). The best binding pose for each ligand was selected according to the lowest binding energy and further analyzed for interactions using Discovery Studio Visualizer [19].

2.8. Molecular Dynamics

Molecular dynamics (MD) simulations were carried out using AMBER 20 to evaluate the stability of ligand-receptor complexes under physiological conditions. The selected complexes—TL49, TL59, and lisinopril bound to the ACE receptor (PDB ID: 1086)—were parameterized using the General Amber Force Field (GAFF) for the ligands and the ff14SB force field for the protein. Each system was solvated in an orthorhombic box of TIP3P water molecules with a minimum buffer distance of 10 Å and neutralized by the addition of Na^+ or Cl^- counterions. Energy minimization was performed in two stages: first with restraints on the protein-ligand complex, followed by an unrestrained minimization. This was followed by gradual heating from 0 K to 310 K over 100 ps under the NVT ensemble, then equilibration for 500 ps under the NPT ensemble. Production MD runs were conducted for 20 ns at 310 K with a 2 fs time step, applying periodic boundary conditions and the particle mesh Ewald method for long-range electrostatics. Trajectories were analyzed using CPPTRAJ to compute the RMSD, Root Mean Square Fluctuation (RMSF), and Molecular Mechanics-Generalized Born Surface Area (MM-GBSA) for binding free energy estimation [20].

3. Results and Discussion

3.1. Target Receptor Identification

The receptor used in this study was the crystal structure of the human ACE in complex with lisinopril (PDB ID: 1086), with a resolution of 2 Å [15]. Receptor quality was assessed using Ramachandran plot statistics, focusing on key parameters such as the most favored regions [A.B.L], which accounted for 93.7%, and disallowed regions [XX], which were 0.0%. These results indicate that the protein structure is of good quality. The 1086 structure includes water molecules, which could complicate the molecular docking simulation. Therefore, receptor preparation involved separating the receptor from its natural ligand, water molecules, and extraneous residues. Removing water molecules was necessary to prevent hydrogen bond formation between water and the ligand, thereby allowing maximal observation of receptor-ligand interactions. The Ramachandran plot statistics are presented in Figure 1.

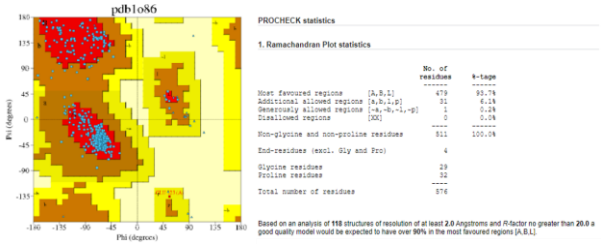

Figure 1. Figure and plot statistics of the Ramachandran 1086 receptor

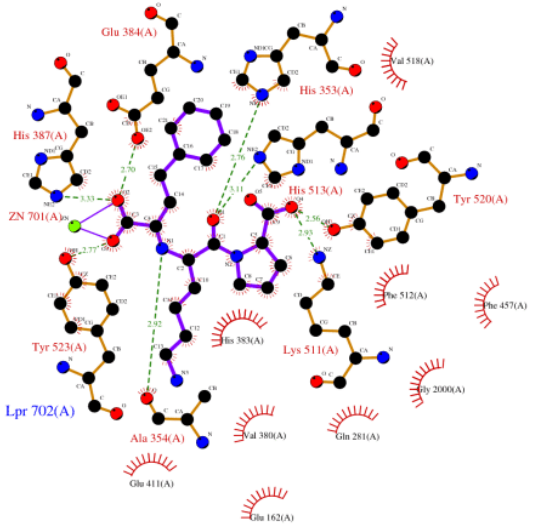

Figure 2. Interaction of the 1086 receptor binding site

Table 1. The example protonation and conformation of luteolin and its derivatives

Compound	Protonation	Conformation
Lisinopril (Reference)	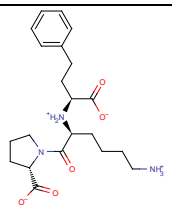	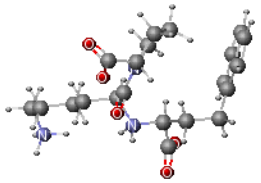
Luteolin	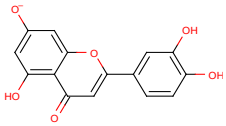	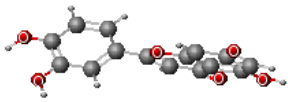
TL1	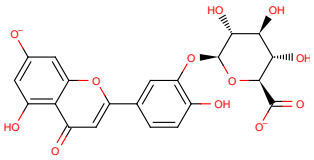	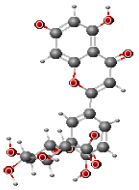
TL2	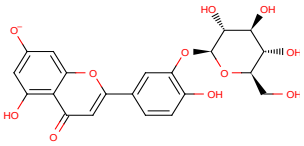	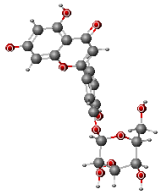
TL3	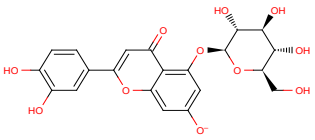	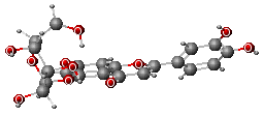
TL4	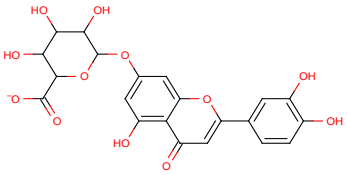	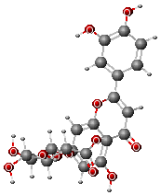
TL5	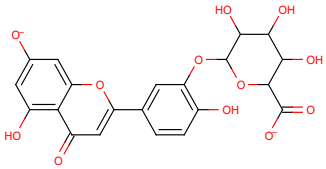	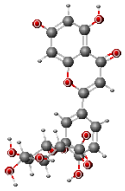
TL6	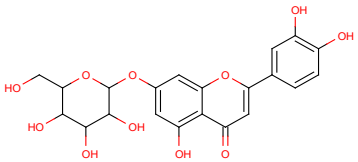	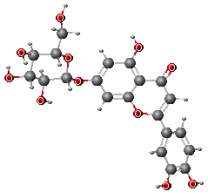
TL7	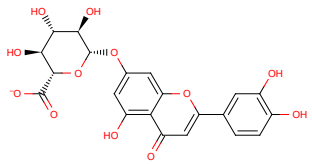	
TL8	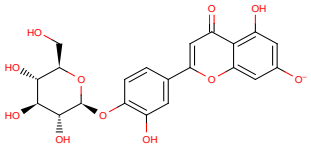	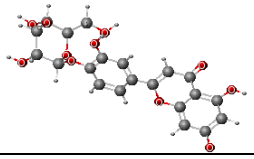

Figure 1 shows that the 1O86 receptor has an active site characterized by hydrogen bonds formed with amino acid residues ALA354, TYR523, HIS387, GLU384, HIS353, HIS513, TYR520, and LYS511. Hydrophobic interactions were observed with VAL518, PHE457, PHE512, GLY2000, GLN281, HIS383, VAL380, GLU162, and GLU411. These interactions at the active site are illustrated in Figure 2.

Compared with the crystal structure of the lisinopril-ACE complex reported by Natesh *et al.* [15], the docking study revealed both consistencies and variations in the key amino acid residues involved in ligand binding. In the original 1O86 structure, lisinopril primarily forms hydrogen bonds with residues such as ALA354, GLU384, HIS353, and TYR523, along with hydrophobic interactions with VAL518 and PHE512. In the redocking simulation, lisinopril maintained interactions with several of these critical residues, particularly GLU384 and LYS118, thereby validating the reliability of the docking protocol. Minor variations in hydrogen bond partners were observed, likely due to differences in ligand conformation and flexibility during the docking process.

Furthermore, the docking simulation did not capture the zinc ion coordination stabilizing lisinopril binding in the crystallographic structure, as PyRx/AutoDock does not explicitly model metal coordination. Nevertheless, the preservation of major active site interactions suggests a strong level of comparability between the in silico approach and the established crystallographic data.

3.2. Docking Validation

Receptor validation was performed by docking or re-docking molecules. The molecular docking results are considered valid if the RMSD value is less than 2.0 Å. A smaller RMSD value indicates better conformation [21]. The receptor validation results for the natural ligand bound to the receptor (PDB ID: 1O86), compared to the crystal structure of the human ACE, show that the natural ligand resides within a grid box of 40 × 40 × 40 Å dimensions, with the grid center coordinates at x = 40.898, y = 32.394, and z = 47.905. The 34th docking run produced an RMSD value of 1.99 Å, with a Gibbs free energy (ΔG) of -8.18 kcal/mol. The ligand position within the grid box is shown in Figure 3.

Figure 3 shows an overlay of the ligand conformation after docking with the original ligand (pre-docking), illustrating that the docked ligand is positioned closely to the original ligand. The overlay comparison between the co-crystallized and redocked lisinopril reveals an RMSD of 1.99 Å, indicating a close but not identical binding pose. The slight differences in orientation can be attributed to the absence of explicit modeling of the catalytic zinc ion in the docking simulation, which plays a crucial role in stabilizing the ligand in the crystal structure. Additionally, docking algorithms such as AutoDock approximate flexibility and electrostatics, which may lead to minor deviations from the experimentally observed poses. Despite these differences, the preservation of key binding site interactions validates the docking protocol.

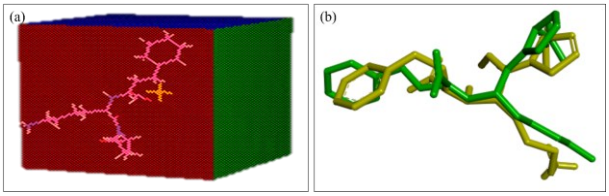

Figure 3. (a) Position of the ligands in the grid box and (b) shape of the natural ligand overlay from the initial 1O86 receptor (green) and after simulated redocking (yellow)

3.3. Ligand Preparation

Ligand preparation involves the processes of drawing, protonation, and conformation for the luteolin compound and its derivatives, as well as lisinopril. Protonation is performed to adjust the ligands to the physiological pH of 7.4, while conformation ensures the ligand is in an appropriate shape to interact with the active site on the receptor [22]. The results of the ligand preparation are presented in Table 1.

3.4. Toxicity and Pharmacokinetics

Toxicity prediction was performed using the PreADMET web server. Toxicity refers to the ability of a chemical to cause harm to organisms, acting as a poison [23]. The toxicity testing aims to assess whether the test compound causes any harmful effects. The toxicity tests include the Ames Test, Carcinogenicity in Mice, and Carcinogenicity in Rats. The Ames Test is used to evaluate the mutagenic potential of a compound. The results of the toxicity screening are presented in Table 2. From Table 2, of the 100 test compounds, only nine compounds passed the toxicity test criteria, meaning they did not cause carcinogenic effects in rats or mice and were not mutagenic. Mutagenic testing is the primary screening method used to identify compounds that may cause DNA mutations, while carcinogenic testing helps determine compounds that could contribute to cancer development.

Pharmacokinetic prediction is performed to assess the presence and activity of active substances in the body, helping to determine their pharmacological effects. The parameters analyzed include CaCo-2 permeability, which predicts the oral permeability of drugs. A good permeability is indicated by a value in the range of 4-70 nm/second. HIA is used to estimate drug absorption in the human small intestine, with values between 70% and 100% indicating good absorption. The PBB parameter is assessed to evaluate drug distribution in the body. A PBB value of <90% suggests weak binding to plasma proteins [24]. The pharmacokinetic prediction results are presented in Table 3.

CaCo-2 permeability (nm/sec) is categorized as follows: <4 indicates low permeability, 4-70 represents medium permeability, and >70 indicates high permeability. %HIA is classified as 0-20% for poor absorption, 20-70% for moderate absorption, and 70-100% for good absorption. %PPB is used to evaluate drug distribution: values >90% suggest strong binding to plasma proteins, while values <90% indicate weak binding.

Table 2. Results of toxicity screening of luteolin and its derivatives

Compound	Toxicity		
	Ames Test	Carcino Mice	Carcino Rats
Lisinopril (Reference)	Non-mutagen	(-)	(+)
Luteolin	Mutagen	(-)	(+)
TL1	Mutagen	(+)	(+)
TL2	Mutagen	(+)	(-)
TL3	Mutagen	(+)	(-)
TL4	Mutagen	(+)	(+)
TL5	Mutagen	(+)	(+)
TL6	Mutagen	(+)	(-)
TL7	Mutagen	(+)	(+)
TL8	Mutagen	(+)	(-)
TL9	Mutagen	(+)	(-)
TL10	Mutagen	(+)	(+)
TL11	Mutagen	(-)	(-)
TL12	Mutagen	(+)	(-)
TL13	Mutagen	(+)	(-)
TL14	Mutagen	(+)	(+)
TL15	Non-mutagen	(-)	(-)
TL16	Mutagen	(+)	(-)
TL17	Mutagen	(-)	(+)
TL18	Mutagen	(+)	(+)
TL19	Mutagen	(+)	(-)
TL20	Mutagen	(+)	(+)
TL21	Mutagen	(+)	(-)
TL22	Mutagen	(+)	(-)
TL23	Mutagen	(-)	
TL24	Mutagen	(+)	(-)
TL25	Mutagen	(+)	(-)
TL26	Non-mutagen	(-)	(-)
TL27	Mutagen	(+)	(+)
TL28	Mutagen	(+)	(+)
TL29	Mutagen	(-)	(-)
TL30	Non-mutagen	(+)	(-)
TL31	Mutagen	(+)	(-)
TL32	Mutagen	(+)	(-)
TL33	Non-mutagen	(-)	(-)
TL34	Mutagen	(+)	(+)
TL35	Mutagen	(-)	(+)
TL36	Non-mutagen	(+)	(-)
TL37	Mutagen	(+)	(-)
TL38	Non-mutagen	(-)	(-)
TL39	Mutagen	(+)	(-)
TL40	Non-mutagen	(+)	(-)
TL41	Non-mutagen	(-)	(+)
TL42	Mutagen	(+)	(-)
TL43	Mutagen	(+)	(+)
TL44	Mutagen	(+)	(-)
TL45	Mutagen	(+)	(-)

Compound	Toxicity		
	Ames Test	Carcino Mice	Carcino Rats
TL46	Non-mutagen	(+)	(-)
TL47	Mutagen	(+)	(+)
TL48	Non-mutagen	(+)	(-)
TL49	Non-mutagen	(-)	(-)
TL50	Non-mutagen	(+)	(-)
TL51	Mutagen	(+)	
TL52	Mutagen	(+)	(-)
TL53	Mutagen	(+)	(+)
TL54	Mutagen	(-)	(-)
TL55	Non-mutagen	(-)	(-)
TL56	Non-mutagen	(-)	(-)
TL57	Non-mutagen	(-)	(+)
TL58	Mutagen	(+)	(-)
TL59	Non-mutagen	(-)	(-)
TL60	Mutagen	(-)	(-)
TL61	Mutagen	(+)	(-)
TL62	Non-mutagen	(+)	(-)
TL63	Non-mutagen	(-)	(-)
TL64	Non-mutagen	(+)	(+)
TL65	Mutagen	(+)	(-)
TL66	Mutagen	(-)	(-)
TL67	Mutagen	(+)	(+)
TL68	Mutagen	(+)	(-)
TL69	Mutagen	(+)	(-)
TL70	Mutagen	(+)	(+)
TL71	Non-mutagen	(+)	(-)
TL72	Mutagen	(+)	(-)
TL73	Mutagen	(+)	(-)
TL74	Mutagen	(+)	(+)
TL75	Non-mutagen	(-)	(-)
TL76	Mutagen	(-)	(-)
TL77	Mutagen	(+)	(-)
TL78	Mutagen	(+)	(-)
TL79	Non-mutagen	(+)	(-)
TL80	Non-mutagen	(+)	(-)
TL81	Mutagen	(+)	(+)
TL82	Non-mutagen	(+)	(-)
TL83	Non-mutagen	(+)	(-)
TL84	Non-mutagen	(+)	(-)
TL85	Non-mutagen	(+)	(-)
TL86	Non-mutagen	(+)	(-)
TL87	Mutagen	(+)	(-)
TL88	Mutagen	(+)	(+)
TL89	Non-mutagen	(+)	(-)
TL90	Non-mutagen	(+)	(-)
TL91	Non-mutagen	(+)	(-)
TL92	Non-mutagen	(+)	(-)
TL93	Mutagen	(+)	(+)
TL94	Non-mutagen	(+)	(+)

Compound	Toxicity		
	Ames Test	Carcino Mice	Carcino Rats
TL95	Mutagen	(+)	(+)
TL96	Non-mutagen	(+)	(-)
TL97	Mutagen	(+)	(-)
TL98	Mutagen	(+)	(+)
TL99	Non-mutagen	(+)	(-)
TL100	Mutagen	(+)	(+)

= Meets toxicity parameters

= Does not meet toxicity parameters

Table 3. Prediction results of the pharmacokinetic aspects of luteolin derivatives

No	Compound	Pharmacokinetics		
		CaCo-2 (nm/sec)	HIA (%)	PPB (%)
1	Lisinopril (Reference)	17.61	72.17	99.71
2	TL15	6.12	5.63	52.17
3	TL26	7.23	1	44.60
4	TL33	2.88	0	40.11
5	TL38	7.14	5.61	47.71
6	TL49	3	1.37	46.86
7	TL55	2.18	0	37.91
8	TL56	5.45	6.66	63.29
9	TL59	23.68	95.86	87.76
10	TL63	6.12	5.63	52.17

= Meet the requirements of pharmacokinetic parameters

= Does not meet the requirements for pharmacokinetic parameters

From Table 3, it can be analyzed that the CaCo-2 value correlates with the permeability of the compound, indicating its ability to penetrate biological membranes. Almost all of the luteolin derivatives tested exhibit moderate permeability, with values ranging from 4 to 70 nm/second. The HIA value reflects the ability of drug compounds to be absorbed in the intestine. HIA prediction is important because, for oral drugs to enter the bloodstream, they must be effectively absorbed through the intestinal wall. The PPB value is related to how drug candidates bind to plasma proteins during distribution. This factor influences the drug concentration available for distribution to various tissues, as only the free (unbound) drug can cross membranes and exert its effects in the body.

3.5. Screening Ligand-Based Drugs Likeness (Drug Scan)

Drug screening was conducted to determine the physicochemical properties of the tested ligands using Lipinski's Rule of Five web server. This rule evaluates five parameters: molecular weight (MW) not exceeding 500 g/mol, logP (coefficient value) less than 5, fewer than five hydrogen bond donors, fewer than 10 hydrogen bond acceptors, and a molar refractivity between 40 and 130 [18]. The results of the drug screening are presented in Table 4.

Molecular weight is associated with the distribution process, where compounds with an MW <500 g/mol can more easily penetrate biological membranes. In contrast, compounds with a molecular weight >500 g/mol face difficulty in crossing cell membranes. The number of hydrogen bond donors and acceptors is linked to the biological activity of a drug molecule. A higher capacity for hydrogen bonding requires more energy for the absorption process to occur [25].

The Log P value (Logarithmic Partition Coefficient) indicates a compound's ability to dissolve in biological fluids. A higher Log P value indicates greater hydrophobicity, which can result in higher toxicity, as hydrophobic compounds tend to accumulate in the lipid bilayer and distribute widely throughout the body, potentially leading to less selective binding to the target enzyme. However, if the Log P value is too negative, the compound may be unable to cross the lipid bilayer membrane [25]. Molar refractivity reflects the total polarization of a drug particle. Non-polar compounds form forces that allow them to bind to receptors, while polar properties help the compound be excreted from the body during the digestive process [16].

3.6. Molecular Docking

Molecular docking is performed on the target protein receptor using PyRx software. The simulations are conducted to determine the interaction conformation of the test compound with the receptor's active site and to identify which test compound exhibits the best binding affinity. Binding affinity measures the potential of a ligand to interact with the target protein [26]. A lower binding affinity indicates a stronger interaction between the receptor and the ligand, while a higher binding affinity suggests a weaker interaction [27].

The molecular docking simulations of luteolin and its derivatives from corn silk were carried out on the 1O86 receptor using the same grid box values as in the redocking validation phase. The docking analysis focuses on selecting the conformation of the compound with the lowest ΔG and inhibition constant (Ki) values [19].

Table 4. Prediction results of the drug scan luteolin derivative test compound

No	Compound	Parameter Lipinski's Rule of Five				
		Molecular weight (< 500 g/mol)	Hydrogen bond donor (<5)	Hydrogen bond acceptor (<10)	Log P (<5)	Molar refractory (40-130)
1	Lisinopril (Reference)	405	0	7	-1.69	105.37
2	TL15	580	2	15	0	0
3	TL26	695	2	19	-7.14	160.78
4	TL33	609	0	16	-4.73	125.56
5	TL38	580	2	15	0	0
6	TL49	447	0	11	-4.15	91.75
7	TL55	641	2	18	-7.68	127.5
8	TL56	463	2	12	-2.41	103.61
9	TL59	449	0	6	0.10	119.09
10	TL63	580	1	15	59.42	477.48

= Fulfills Lipinski's rules

= Does not comply with Lipinski's rules

Table 5. Molecular docking results of luteolin derivative test compounds

No	Compound	Binding energy (kcal/mol)	Ki (μM)	Run
1	Lisinopril (Reference)	-6.33	22.92	33
2	TL15	-5.69	67.67	94
3	TL26	-3.27	3.98	87
4	TL33	-5.28	135.42	4
5	TL38	-6.98	17.74	17
6	TL49	-6.07	35.52	83
7	TL55	-4.24	776.61	80
8	TL56	-5.98	41.54	84
9	TL59	-9.10	0.211	16
10	TL63	-6.06	36.14	9

Free binding energy, or Gibbs free energy (ΔG), reflects the ability of a drug to bind to a receptor. A lower ΔG value indicates stronger binding affinity between the receptor and the ligand, whereas a higher ΔG value suggests weaker binding. The more negative the ΔG value, the better the affinity. The Ki is directly related to ΔG; a lower Ki value corresponds to a stronger binding interaction between the ligand and receptor. The results of the molecular docking of the luteolin derivative test compounds are presented in Table 5.

Based on the results from toxicity screening, pharmacokinetics, drug scanning, and molecular binding of the luteolin derivative test compounds to the 1O86 receptor, two compounds were identified with low ΔG and Ki values: compound TL49, with a binding energy of -6.07 kcal/mol, and compound TL59, with a binding energy of -9.10 kcal/mol. This indicates that TL59 has a stronger affinity for the 1O86 receptor than TL49 and the reference drug, lisinopril. Consequently, TL59 is predicted to have stable and favorable interactions with the 1O86 receptor, suggesting it may be a better candidate for antihypertensive therapy than lisinopril.

Table 6. Interaction results of molecular docking of luteolin derivative test compounds

Compound	Interaction with amino acids	
	Hydrogen bonds	Hydrophobic bonding
Lisinopril (Reference)	LYS118, GLU403, GLU123	TYR360, ARG522, MET223, HIS410, GLY404
Natural ligand	ALA354, TYR523, HIS387, GLU384, HIS353, TYR520, LYS511	VAL518, PHE457, PHE512, GLY200, GLN281, HIS383
TL49	ASP358, TYR360, ASN70	PHE391, ALA356, TYR62, TRP357, SER355, VAL351
TL59	ASP453, LYS454, GLU384, ALA354, CYS370, THR372, ASP 377	VAL3789, HIS353, THR, 166, ALA170, GLU162,

In addition to ΔG and the Ki, molecular docking also provides insights into ligand-receptor interactions at the active site, which are critical for determining the stability of the complex. The analysis primarily focuses on hydrogen bonds, as these are common in human biological systems, although hydrophobic interactions are also essential in maintaining the stability of ligand-receptor binding [28]. The interaction results from the molecular docking of TL59 and lisinopril with the 1O86 receptor are presented in Table 6.

The results of the molecular docking, visualized in two-dimensional form (Figure 4), highlight the hydrogen and hydrophobic bonds formed between the molecules. Hydrogen bonds significantly influence the stability of ligand-receptor interactions, with an increase in binding energy indicative of stronger interactions between the ligand and the receptor [29].

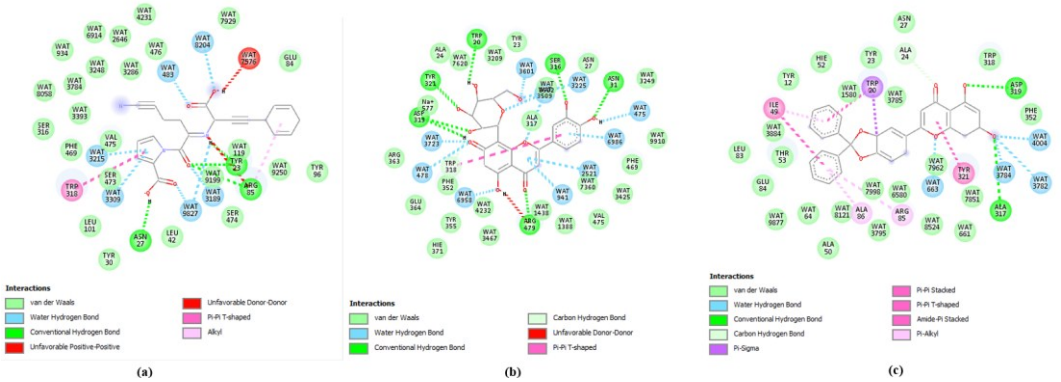

Figure 4. 2D visualization of the best binding poses based on free energy values: (a) lisinopril (reference), (b) compound TL49, and (c) compound TL59

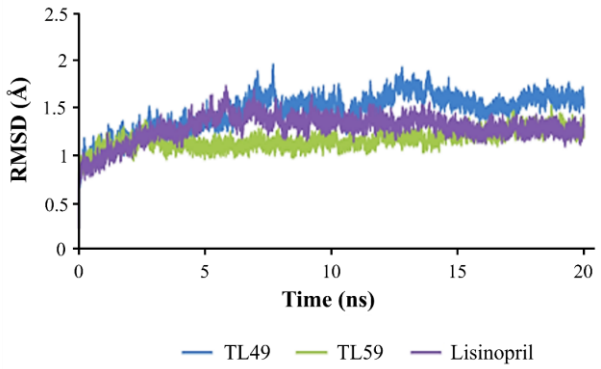

Figure 5. The RMSD graph

In the 1O86 receptor (natural ligand), key hydrogen bond interactions at the active site involve the amino acid residues ALA354 and GLU384. Similar interactions are observed with the TL59 compound and the receptor. The overlap in binding residues between TL59 and the receptor suggests that TL59 effectively interacts at the active site, potentially exhibiting activity comparable to the co-crystallized ligand. These binding site residues are critical for stabilizing the ligand and modulating receptor function.

3.7. Molecular Dynamics

Based on the results of toxicity screening, pharmacokinetics, drug scans, and molecular docking of 100 luteolin derivative test compounds, two compounds, TL49 and TL59, were selected due to their favorable ΔG values of -6.07 kcal/mol and -9.10 kcal/mol, respectively. These compounds will undergo molecular dynamics simulations to assess the stability of their interactions with the receptor. Molecular dynamics simulations, performed using AMBER software, include three compounds: lisinopril and the two selected test compounds, TL49 and TL59. These compounds were chosen based on their favorable binding energy values from initial screening. The simulations will evaluate the dynamic properties of ligand-receptor interactions, including temperature, pressure, and interactions over specified time intervals [20]. The results of the molecular dynamics simulation were analyzed to observe the changes in the ligand-receptor complex over time and to assess the stability of the complex structure. This analysis was carried out using key parameters, including RMSD, RMSF, and MM-GBSA.

3.7.1. Root Mean Square Deviation (RMSD)

RMSD is a parameter used to measure distance changes and ligand conformations in three-dimensional geometry. The RMSD value is calculated by comparing the initial ligand conformation with the conformation during simulation, presented in graphical form and plotted over time [20]. The RMSD values from the simulation results, expressed in angstroms (Å), are shown in Figure 5.

Based on Figure 5, during the 20 ns simulation, TL49, TL59, and lisinopril all showed an increase in RMSD at the start of the simulation. TL59 maintained stability from 5 ns to 18 ns, with an RMSD around 1 Å, followed by a slight increase between 19 ns and 20 ns. For lisinopril, the ligand-receptor complex exhibited unstable interactions until approximately 15 ns, after which stability was achieved from 16 ns to 20 ns with an RMSD value around 1.3 Å. Meanwhile, TL49 displayed an interaction pattern similar to lisinopril but did not reach a stable state within the 20 ns timeframe, indicating that a longer simulation time may be needed. The TL59 compound demonstrated better stability than TL49 and lisinopril, as indicated by its consistently lower RMSD values. This suggests that the 1O86 receptor exhibits better flexibility and more stable interactions with the TL59 compound.

3.7.2. Root Mean Square Fluctuation (RMSF)

RMSF is a measure of the deviation of a particle's position relative to a reference position. The fluctuation value is calculated by assessing the extent to which the protein residues move during the simulation process [20]. RMSF can also be used to predict regions of protein flexibility by illustrating conformational changes in the protein chain throughout the simulation time [30]. Low fluctuation values in the residues indicate low adaptability and a stable connection in ligand-receptor binding, whereas high fluctuation values suggest high adaptability and a less stable interaction due to frequent positional changes during the simulation. The RMSF values from the simulation results, expressed in angstroms (Å), are shown in Figure 6.

Based on Figure 6, it can be seen that the fluctuations of TL49, TL59, and lisinopril show almost the same fluctuation movements. The amino acid residue that experienced high fluctuations was the TL49 compound on the ASP105 amino acid residue, and the lowest fluctuation was the TL59 compound on the ASP37 amino acid residue.

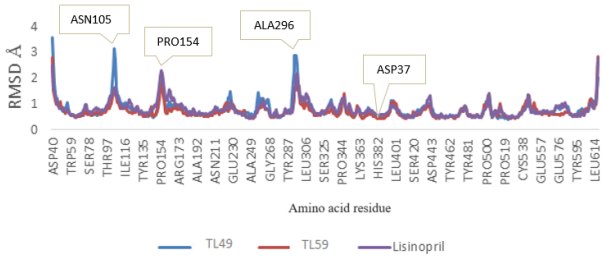

Figure 6. The RMSF Graph

The RMSF graph shows an increase in fluctuations in the 1O86 amino acid residue with the TL49 compound, the TL59 compound, and the lisinopril compound. In the TL59 compound, the highest fluctuation was the PRO154 amino acid residue, but this amino acid did not play an important role as an active site. Better fluctuations can be shown by lower fluctuations, namely the ASP377 amino acid residue, which shows that the interaction of the TL59 compound with the 1O86 receptor has better binding. The analysis was carried out using Discovery Studio software on the selected test compounds and lisinopril to see the position of the ligand and protein. It can be seen in Figure 7 that the movement of ligands and proteins resulting from the visualization of the lisinopril compound with the TL59 compound produces good or stable interactions.

The superimposition results illustrate the changes in the ligand's position relative to the protein during the molecular dynamics simulation. A closer alignment between the ligand and the protein indicates a stronger and more stable interaction.

3.7.3. Molecular Mechanics-Generalized Born Surface Area (MM-GBSA)

The free energy (ΔG) obtained through the MM-GBSA calculation method reflects the binding affinity of a compound to its receptor. A lower ΔG value indicates a stronger ability of the compound to bind to the receptor [31]. Among the three compounds tested through molecular dynamics simulations—compound TL49, compound TL59, and lisinopril—the MM-GBSA results are seen in Table 7.

Table 7. Results of free binding energy calculations for ligand–receptor systems of selected luteolin derivative test compounds

Energy (kcal/mol)	TL49	TL59	Lisinopril
VDWAALS	-32.69	-55.45	-41.47
EEL	305.41	153.9	218.68
EGB	-5.30	-5.44	-5.03
ΔG_{gas} (VdW+EEL)	272.72	98.45	177.20
ΔG_{solv} (EGB + ESURF)	-280.53	-143.11	-206.45
ΔG_{TOTAL} (VdW + EEL + EGB + ESURF)	-7.81	-44.65	-29.25

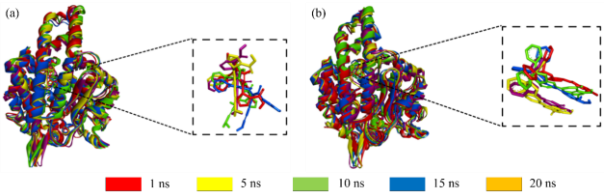

Figure 7. Superimposition of the molecular dynamics simulation results: (a) lisinopril–1O86 complex and (b) TL59–1O86 complex

Based on Table 7, it can be observed that the ΔG_{TOTAL} value obtained from the MM-GBSA calculations for the TL59 compound system is lower at -44.65 kcal/mol compared to TL49 (-7.81 kcal/mol) and the reference compound, lisinopril (-29.25 kcal/mol). This indicates that TL59 has a better binding affinity and greater stability than both TL49 and the reference compound. Therefore, TL59 is predicted to be a promising antihypertensive drug candidate targeting the ACE receptor (PDB ID: 1O86). TL59 is proposed to exert its antihypertensive effect by inhibiting the conversion of angiotensin I to angiotensin II, thereby reducing peripheral vascular resistance and lowering blood pressure [32].

4. Conclusion

Based on the research conducted, it can be concluded that out of the 100 luteolin-derived test compounds from corn silk (*Zea mays* L.), only nine compounds met the requirements for toxicity, pharmacokinetics, and Lipinski's Rule of Five through in silico screening. The interaction between the luteolin derivatives and the ACE receptor involved hydrogen bonds and hydrophobic interactions. Notably, key hydrogen bond interactions were observed with the amino acid residues ALA354 and GLU384, suggesting that the TL59 test compound may exhibit similar biological activity by binding to the same critical residues. TL59 demonstrated the best potential as an antihypertensive drug candidate in silico, with a lower molecular docking free energy (ΔG) of -9.10 kcal/mol compared to the reference compound (-6.33 kcal/mol). Furthermore, the MM-GBSA free energy calculation revealed that TL59 exhibited a lower total free energy (ΔG_{TOTAL}) of -44.65 kcal/mol compared to the control compound (-29.25 kcal/mol). These findings highlight TL59 as a promising lead compound for antihypertensive drug development targeting ACE. However, since this study was limited to computational predictions, future research should involve in vitro enzyme inhibition assays, cell-based functional studies, and in vivo validation to confirm the efficacy, bioavailability, and safety profile of TL59 in biological systems.

Acknowledgments

The author thanks the Perjuangan Tasikmalaya University for providing facilities for this research.

References

[1] Tori Rihiantoro, Muji Widodo, Hubungan Pola Makan dan Aktivitas Fisik dengan Kejadian Hipertensi di Kabupaten Tulang Bawang, *Jurnal Ilmiah Keperawatan Sai Betik*, 13, 2, (2017), 159-167 https://doi.org/10.26630/jkep.v13i2.924

[2] World Health Organization, Hypertension, (2023), [accessed on 15 Feb 2022] https://www.who.int/news-room/fact-sheets/detail/hypertension

[3] Kementerian Kesehatan RI, Hipertensi Penyebab Utama Penyakit Jantung, Gagal Ginjal, dan Stroke, (2021), [accessed on 18 Feb 2023]

[4] Dinas Kesehatan Provinsi Jawa Barat, Profil Kesehatan Jawa Barat Tahun 2021, [accessed on 18 Feb 2023], (2021), 120-121 https://app-diskes.jabarprov.go.id/drive/s/P65z6fRg5sCrmzX

[5] Anita Lufianti, Sutrisno Sutrisno, The Effectiveness Relaxation Therapy of Imagination Guided Reduction Blood Pressure on Elderly With Hypertension in the Working Area Health Center Purwodadi 1 Grobogan Regency, *Media Keperawatan Indonesia*, 2, 2, (2019), 73-78 https://doi.org/10.26714/mki.2.2.2019.25-30

[6] Putri Kristanti, Efektifitas dan Efek Samping Penggunaan Obat Antihipertensi Pada Pasien Hipertensi di Puskesmas Kalirungkut Surabaya, *CALYPTRA: Jurnal Ilmiah Mahasiswa Universitas Surabaya*, 4, 2, (2016), 1-13

[7] Yance Anas, Naimi Amalia Hatimah, Efek antihipertensi ekstrak etanol kombinasi rambut dan biji jagung (*Zea mays* L.) pada tikus hipertensi yang diinduksi monosodium glutamat, *Jurnal Ilmu Farmasi dan Farmasi Klinik*, 15, 1, (2018), 29-36 https://doi.org/10.31942/jiffk.v15i01.2170

[8] Kristover Koloay, Gayatri Citraningtyas, Widya Astuty Lolo, Uji efektivitas ekstrak etanol rambut jagung (*Zea mays* L.) terhadap penurunan kadar gula darah tikus putih jantan galur wistar (*Rattus norvegicus* L.) yang diinduksi aloksan, *PHARMACON: Jurnal Farmasi Indonesia*, 4, 3, (2015), 34-40

[9] David Albert Pangemanan, Edi Suryanto, Paulina V. Y. Yamlean, Skrinning Fitokimia, Uji Aktivitas Antioksidan dan Tabir Surya pada Tanaman Jagung (*Zea mays* L.), *PHARMACON*, 9, 2, (2020), 194-204 https://doi.org/10.35799/pha.9.2020.29271

[10] Ligia Guerrero, Julián Castillo, Mar Quiñones, Santiago Garcia-Vallvé, Lluis Arola, Gerard Pujadas, Begoña Muguerza, Inhibition of Angiotensin-Converting Enzyme Activity by Flavonoids: Structure-Activity Relationship Studies, *PLOS ONE*, 7, 11, (2012), e49493 https://doi.org/10.1371/journal.pone.0049493

[11] Hendra Herman, Bayu Putra, Uji Antihipertensi Infus Kombinasi Biji dan Rambut Jagung (*Zea mays* L.) pada Tikus Jantan (*Rattus norvegicus*) dengan Metode Tail Cuff Non Invasive, *Jurnal Media Farmasi*, 12, 1, (2015), 93-103 https://doi.org/10.12928/mf.v12i1.3027

[12] Gladys O. George, Faustina K. and Idu, Corn silk aqueous extracts and intraocular pressure of systemic and non - systemic hypertensive subjects, *Clinical and Experimental Optometry*, 98, 2, (2015), 138-149 https://doi.org/10.1111/cxo.12240

[13] Yance Anas, Ika Nilam Cahyani, Ulum Firnanda Sukma, Efektivitas Fraksi Aktif Ekstrak Etanol Labu Siam (*Sechium Edule* (Jack) Sw) Sebagai Antihipertensi Pada Tikus Hipertensi Yang Diinduksi Monosodium Glutamat, *Jurnal Ilmu Farmasi dan Farmasi Klinik*, 18, 01, (2021), 1-7 https://doi.org/10.31942/jiffk.v18i01.4893

[14] Yohanes Bare, Andri Maulidi, Dewi Ratih Tirto Sari, Sri Sulystyaningsih Natalia Daeng Tiring, Studi in Silico Prediksi Potensi 6-Gingerol sebagai inhibitor c-Jun N-terminal kinases (JNK): Prediction Potential of 6-gingerol as c-Jun N-terminal kinases (JNK): In Silico approach, *Jurnal Jejaring Matematika dan Sains*, 1, 2, (2019), 59-63 https://doi.org/10.36873/jjms.v1i2.211

[15] Ramanathan Natesh, Sylva L. U. Schwager, Edward D. Sturrock, K. Ravi Acharya, Crystal structure of the human angiotensin-converting enzyme–lisinopril complex, *Nature*, 421, 6922, (2003), 551-554 https://doi.org/10.1038/nature01370

[16] Richa Mardianingrum, Kamiel Roesman Bachtiar, Susanti Susanti, Aas Nuraisah Aas Nuraisah, Ruswanto Ruswanto, Studi in silico senyawa 1, 4-Naphthalenedione-2-Ethyl-3-Hydroxy sebagai antiinflamasi dan antikanker payudara, *ALCHEMY Jurnal Penelitian Kimia*, 17, 1, (2021), 83-95 https://doi.org/10.20961/alchemy.17.1.43979.83-95

[17] Susanti N. M. P., Warditiani N. K., Dewi K. A. S., Oka M., Aktivitas Antihiperlipidemia Andrografolid dari Sambiloto (*Andrographis paniculata* (Burm. f.) Ness) secara *In Silico*, *Jurnal Farmasi Udayana*, 5, 2, (2017), 58-62

[18] Ruswanto Ruswanto, Richa Mardianingrum, Tresna Lestari, Tita Nofianti, Lilis Tuslinah, Dudi Nurmalik, In silico study of the active compounds in bitter melon (*Momordica charantia* L) as antidiabetic medication, *Pharmaciana*, 8, 2, (2018), 177-194

[19] Kartika Juliana, Mohamad Amin, Endang Suarsini, Analisis *Virtual Screening* Senyawa Alami Anti Aging Kandidat Inhibitor Komplek Protein Mmp1, *Prosiding SNPBS (Seminar Nasional Pendidikan Biologi dan Saintek)*, 2016

[20] Rizka Amalia, Ruswanto Ruswanto, Molecular Dinamik Senyawa Turunan Benzimidazol Sebagai Inhibitor Kolinesterase, *Prosiding Seminar Nasional dan Penelitian Kesehatan 2018*, 2019

[21] Fauzan Zein Muttaqin, Muhammad Ferdian Pratama, Fransiska Kurniawan, Molecular docking and molecular dynamic studies of stilbene derivative compounds as sirtuin-3 (SIRT3) histone deacetylase inhibitor on melanoma skin cancer and their toxicities prediction, *Journal of Pharmacopolium*, 2, 2, (2019), 112-121

[22] I. R. Hartanti, A. A. Putri, N. N. Auliya AS, A. L. Triadenda, E. Laelasari, C. Suhandi, M. Muchtaridi, Molecular Docking Senyawa Xanton, Benzofenon, dan Triterpenoid sebagai Antidiabetes dari Ekstrak Tumbuhan Garcinia Cowa, *Jurnal Kimia (Journal of Chemistry)*, 16, 1, (2022), 72-83 https://doi.org/10.24843/JCHEM.2022.v16.i01.p10

[23] Muh Fitrah, Nurshalati Tahar, Husniar Husniar, Uji Toksisitas Fraksi Daun Pedada (*Sonneratia caseolaris* L.) Tehadap Larva Udang (Artemia salina leach) dengan Menggunakan Metode *Brine Shrimp Lethality Test* (BSLT), *Parapemikir: Jurnal Ilmiah Farmasi*, 7, 1, (2018), 181-186 https://doi.org/10.30591/pjif.v7i1.739

[24] Ruswanto Ruswanto, Mardhiah Mardhiah, Richa Mardianingrum, Korry Novitriani, Sintesis dan Studi *In Silico* Senyawa *3-Nitro-N'-[(Pyridin-4-Yl) Carbonyl] Benzohydrazide* sebagai Kandidat

Antituberkulosis, *Chimica et Natura Acta*, 3, 2, (2015), 54-61 https://doi.org/10.24198/cna.v3.n2.9183

[25] Christopher A. Lipinski, Lead-and drug-like compounds: the rule-of-five revolution, *Drug Discovery Today: Technologies*, 1, 4, (2004), 337-341 https://doi.org/10.1016/j.ddtec.2004.11.007

[26] Sargis Dallakyan, Arthur J. Olson, Small-Molecule Library Screening by Docking with PyRx, in: J.E. Hempel, C.H. Williams, C.C. Hong (Eds.) *Chemical Biology: Methods and Protocols*, Springer New York, New York, NY, 2015, https://doi.org/10.1007/978-1-4939-2269-7_19

[27] Karisma Enggar Saputri, Nurul Fakhmi, Erwinda Kusumaningtyas, Dedy Priyatama, Broto Santoso, Docking molekular potensi anti diabetes melitus tipe 2 turunan zerumbon sebagai inhibitor aldosa reduktase dengan autodock-vina, *Chimica et Natura Acta*, 4, 1, (2016), 16-20 https://doi.org/10.24198/cna.v4.n1.10443

[28] Arwansyah Arwansyah, Laksmi Ambarsari, Tony I. Sumaryada, Simulasi *docking* senyawa kurkumin dan analognya sebagai inhibitor reseptor androgen pada kanker prostat, *Current Biochemistry*, 1, 1, (2014), 11-19

[29] Puji Astuty, Noer Komari, Kajian *Molecular Docking* Senyawa *Karwinaphthol B* dari Tanaman Bawang Dayak (*Eleutherine palmifolia* (L.) Merr) sebagai Inhibitor Enzim Glukokinase, *Jurnal Natural Scientiae*, 2, 1, (2022), 01-09 https://doi.org/10.20527/jns.v2i1.5412

[30] Oyinlola Oluwunmi Olaokun, Sizakele Annousca Manonga, Muhammad Sulaiman Zubair, Saipul Maulana, Nqobile Monate Mkolo, Molecular Docking and Molecular Dynamics Studies of Antidiabetic Phenolic Compound Isolated from Leaf Extract of *Englerophytum magalismontanum* (Sond.) T.D.Penn, *Molecules*, 27, 10, (2022), 3175 https://doi.org/10.3390/molecules27103175

[31] G. Lizbeth Ramírez-Salinas, Jazmín García-Machorro, Saúl Rojas-Hernández, Rafael Campos-Rodríguez, Arturo Contis-Montes de Oca, Miguel Medina Gomez, Rocío Luciano, Mirko Zimic, José Correa-Basurto, Bioinformatics design and experimental validation of influenza A virus multi-epitopes that induce neutralizing antibodies, *Archives of Virology*, 165, 4, (2020), 891-911 https://doi.org/10.1007/s00705-020-04537-2

[32] Wilbert S. Aronow, Jerome L. Fleg, Carl J. Pepine, Nancy T. Artinian, George Bakris, Alan S. Brown, Keith C. Ferdinand, Mary Ann Forciea, William H. Frishman, Cheryl Jaigobin, John B. Kostis, Giuseppi Mancia, Suzanne Oparil, Eduardo Ortiz, Efrain Reisin, Michael W. Rich, Douglas D. Schocken, Michael A. Weber, Deborah J. Wesley, ACCF/AHA 2011 Expert Consensus Document on Hypertension in the Elderly, *Circulation*, 123, 21, (2011), 2434-2506 https://doi.org/10.1161/CIR.0b013e31821daaf6